Available online at www.sciencedirect.com
SCIENCE DIRECT®
Journal of the European Ceramic Society 25 (2005) 589–597
www.elsevier.com/locate/jeurceramsoc

Mechanical properties and mechanical behaviour of SiC dense-porous laminates

C. Reynaud [a], F. Thévenot [a], T. Chartier [b,*], J.-L. Besson [b]

[a] *Dept. Céramiques Spéciales, E.N.S. des Mines de Saint-Etienne, 42023 Saint-Etienne, France*
[b] *S.P.C.T.S., U.M.R. C.N.R.S. 6638, E.N.S. de Céramiques Industrielles, 87065 Limoges, France*

Received 3 December 2003; received in revised form 23 February 2004; accepted 28 February 2004

Available online 15 June 2004

Abstract

Porous laminar materials and alternate laminates of silicon carbide dense and porous layers have been elaborated by tape casting and liquid phase sintering processing. Porosity was introduced by incorporation of pore forming agents (corn starch or graphite platelets) in the slurry. Homogeneous distributions of porosity have been obtained for both monolithic and composite laminates. The microstructure of the SiC matrix was equiaxed and was not affected by the porosity. The porosity (P) dependence of Young's modulus (E), modulus of rupture (σ_R), toughness (K_{1C}) and fracture energy (G_{1C}) was found to be well described on the entire range of porosity by relations of the form $X_0(1-P)^{mX}$ proposed by Wagh et al. from a model that takes into account the tortuosity of the porosity. In the case of our materials, $m_E = 2.7$, $m_{\sigma_R} = m_{K_{1C}} = m_E + 0.5$ and $m_{G_{1C}} = m_E + 1$. All the ex-corn starch composites behaved in a brittle manner, even those having weak interlayers with a porosity content higher than the critical value of about 0.4 predicted by the model developed by Blanks et al. A non-purely brittle behaviour started to be obtained with ex-graphite laminar composites in which the pores are elongated and oriented parallel to the interfaces.

Keywords: Composites; Porosity; Mechanical properties; SiC; Laminates

1. Introduction

Among the strategies developed to improve the flaw tolerance of non-transforming ceramics, the designing of laminar structures with weak interfaces or interphases promoting crack deflection mechanisms have proved to be a successful way to increase fracture energy. The weak interfaces most commonly used are either graphite[1] or boron nitride.[2,3] For instance, in the case of graphite interfaces, Clegg et al. have obtained an apparent toughness and a fracture energy respectively 5 and 200 times higher than the typical values of monolithic α-SiC.[1] However, since graphite and boron nitride have a low oxidation resistance and cannot be used at high temperature in oxidising atmosphere without a protective barrier, other systems have been investigated, specially with oxidation resistant weak interphases such as monazite,[4] fluorophlogopite[5] or $MoSi_2 + Mo_2B_5$.[6]

As a necessary condition for the interfacial material is that it must be chemically compatible with the material of the strong layers, Clegg and co-workers studied ceramic laminates with alternating dense and porous layers made of silicon carbide[7] or alumina.[8] This approach has also the advantage of avoiding the building up of any internal stresses due to difference in thermal expansion coefficients which can be the source of delamination during cooling.[9]

According to theoretical analysis by He and Hutchinson of the kinking of a crack out of an interface,[10] crack deflection is to occur when the ratio between the fracture energy of the homogeneous weak interphase, G_i, and the fracture energy of the strong layer, G_S, is lower than 0.57. However, in the case of dense-porous laminates, the porous layer is inhomogeneous, and the fracture energy to be considered is that of the ligament of matter between the crack and the pore ahead of it, G_{lig}[7]. Than the criterion for crack deflection in the weak interphase becomes $G_{lig}/G_S < 0.57$. Though these ligaments of matter are made of the same material as the dense layers, and might be expected to have the same fracture energy, theoretical analyses show that if the tip of a

* Corresponding author.
E-mail address: t.chartier@ensci.fr (T. Chartier).

0955-2219/$ – see front matter © 2004 Published by Elsevier Ltd.
doi:10.1016/j.jeurceramsoc.2004.02.009

growing crack comes sufficiently close to a microcrack[11] or a pore,[12] the stress intensity factor at the tip of the crack is increased and then, the apparent fracture energy of the ligament is reduced. This reduction varies with the relative density, and for a cubic array of spherical pores, Blanks et al.[7] derived a minimum level of porosity equal to 37% to ensure crack deflection, in good agreement with their experimental results for silicon carbide. Assuming that the fracture energy of the dense ligament is related to that of the porous layer, G_P, by the relation:

$$G_{lig} = \frac{G_P}{1 - P} \quad (1)$$

where P is the volume fraction of porosity, Davis et al.[8] expressed the criterion for continued crack deflection in terms of easily measurable variables:

$$\frac{G_P}{G_S} < 0.57(1 - P) \quad (2)$$

The experimental results obtained by Clegg's group with either alumina or silicon carbide were consistent with relation (2), crack deflection being observed when the ratio G_P/G_S falls under the line $0.57(1 - P)$, that occurs for a volume fraction of porosity of 0.37.

The aim of the work presented in this paper was to determine the porosity dependence of the mechanical properties of a SiC material densified by liquid phase sintering on a wide range of porosity, and to compare the mechanical behaviour of dense-porous laminates to that obtained by Blanks et al.[7] for silicon carbide densified by solid state sintering.

2. Processing and materials microstructure

2.1. Processing

The materials were made by stacking layers obtained by tape casting and co-sintering. The ceramic powder must have a narrow particle size distribution and a rather low mean diameter d_{50} was 1 μm for the starting α-SiC powder (Sika Tech FCP13, Norton-Norway) and the specific surface area (BET) was 13 m^2/g. The densification aids (5 wt.% of the total ceramic content) for the liquid phase sintering of SiC were Y_2O_3 (Rhone-Poulenc-France) and Al_2O_3 (CR15 Baïkowski-France) in a ratio corresponding to the YAG–Al_2O_3 eutectic composition (40 wt.% Y_2O_3–60 wt.% Al_2O_3).

The first step of the elaboration of the suspensions for tape-casting consists in the dispersion of the ceramic powders in a solvent containing a dispersant. This was performed by planetary milling with alumina balls during 4 h in the MEK-ethanol azeotrope containing 0.6 wt.% of a phosphate ester (CP213, Cerampilot-France). Then, an acrylic binder (Degalan® LP51/01, Röhm and Haas-US) and a phtalate plasticizer (DPB, Prolabo-France) were added to the suspension and mixed during 16 h. They allow to optimise the viscosity and the rheological behaviour of the slurry and complement one another to produce handleable ceramic tapes. The optimum concentrations for the binder and the plasticizer were determined to be 8 wt.% for both additives on the base of the ceramic powder. The third step corresponds to the incorporation, into the suspension, of the pore forming agent (PFA): corn starch (Roquette-France) or graphite platelets (Union Carbide-US) (Table 1). The PFA volume fraction, referred to the sum of the ceramic volume and PFA volume, was 45 and 50% for graphite platelets and varied from 5 to 55% for corn starch. We were unable to fabricate sound parts when larger PFA volume fraction were incorporated. A mixing time of 3.5 h leads to an uniform distribution of the PFA. Finally the slurry was de-aired at a low rotation speed during 24 h.

Table 1
Characteristic parameters of the two PFAs used

	PFA	
	CS	GP
Chemical nature	Corn starch	Graphite platelet
Dimension	$d_{50} = 14\,\mu m$	$8\,\mu m \times 8\,\mu m \times 3\,\mu m$
Aspect ratio	1.2	2.67

Then the slurries were tape cast onto a Mylar® film using a moving double blade device on a laboratory tape casting bench (Elmeceram-France). The tapes had smooth surfaces and uniform thicknesses, which could be varied between 100 and 150 μm. Sheets were punched in the green tapes and stacked on each other using two types of stacking sequence: (i) stacking of identical layers to obtain monolithic dense or porous specimens, and (ii) alternate stacking of PFA free and PFA containing layers to obtain symmetrical dense/porous laminar composites. The outer layers were always dense layers. The number of tapes was chosen to lead to a final thickness of about 3–4 mm after sintering. The thickness of the layers was varied by stacking several tapes of the same nature. This led to different architectures that allowed to study the influence of the dense to porous thickness ratio.

After stacking, the specimens were pressed under 60 MPa at 65 °C. The burnout of organics was performed by heating very slowly (6 °C/h) up to 550 °C in air. Sintering was conducted in a graphite furnace (VAS, France) under argon at atmospheric pressure during 1 h at 1950 °C. The relative density of the PFA free monolithic specimens was 98%.

2.2. Microstructure

A detailed description of the sintered microstructures of the monolithic and laminated SiC materials have been already published.[13] So, only the main results will be briefly reported here.

The microstructures were homogeneous, and in the case of the laminar composites, the layers were parallel with an

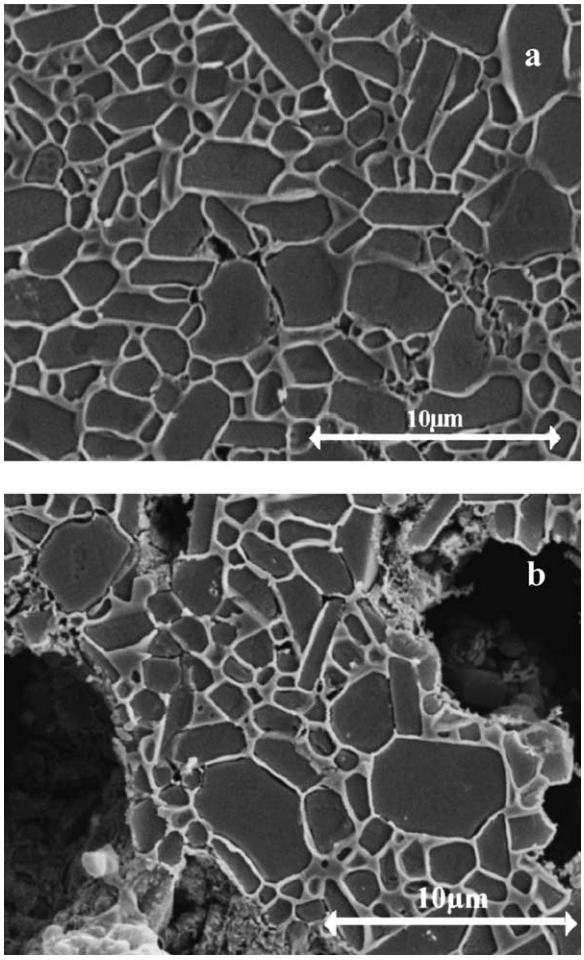

Fig. 1. SEM micrographs; grain microstructure revealed by plasma etching. (a) Dense SiC, (b) porous SiC obtained by the incorporation of 45 vol.% corn starch.

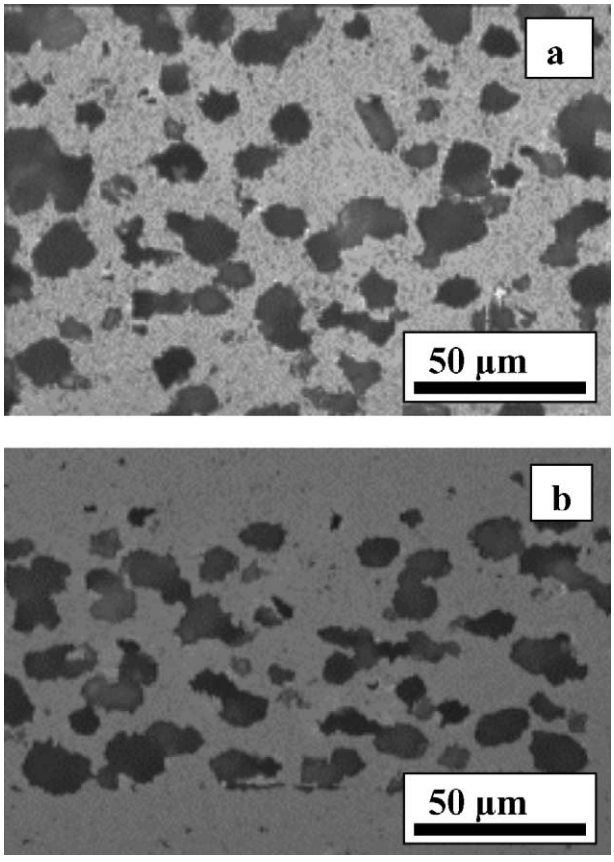

Fig. 2. Optical micrographs showing the morphology of the porosity. (a) Monolithic laminate, (b) laminar composite.

uniform thickness. The thickness was about 70 μm for the dense layers, 80–90 μm for the ex-corn starch porous layers and 20–30 μm for the porous layers where graphite platelets were used. No migration of pores from porous to dense layers was observed. Dense layers and skeletons in the porous layers were constituted by the same homogeneous, fine and equiaxed microstructure with a mean equivalent diameter of about 1.25 μm (Fig. 1). The pore characteristics were the same in the porous layers of the laminates and in their monolithic counterparts (Fig. 2). Whereas the pores introduced by corn starch had a low aspect ratio, those coming from graphite platelets were elongated and mostly oriented parallel to the interfaces (Fig. 3). The porosity of the monoliths reached a maximum and levelled off for corn starch amounts higher than 40%. When the porous layers were co-sintered with dense layers, the amount of final porosity followed the law established by Slamovich and Lange[14] for thermodynamically stable pores shrinking the same amount as the matrix (Fig. 4). The lower shrinkage of the dense layers introduced tensile internal stresses in the highest porous layers. However, the difference in volumetric shrinkage between the porous monoliths and the corresponding porous layers in the laminates remained low, that allowed the properties of the porous layers to be obtained from tests on their monolithic counterparts without introducing a noticeable error.

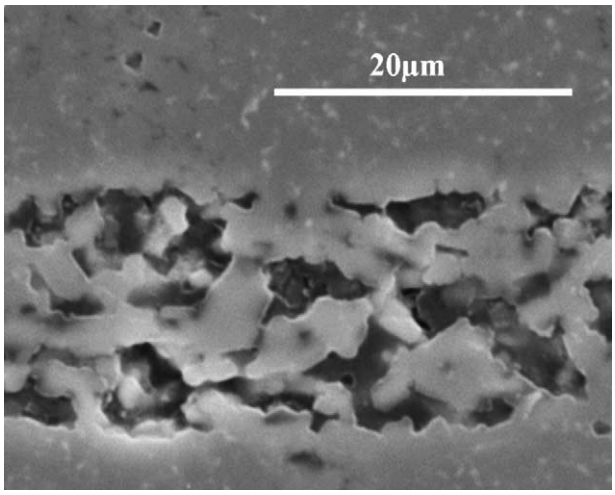

Fig. 3. Optical micrograph showing the morphology of the porosity resulting from the incorporation of 50 vol.% of graphite platelets.

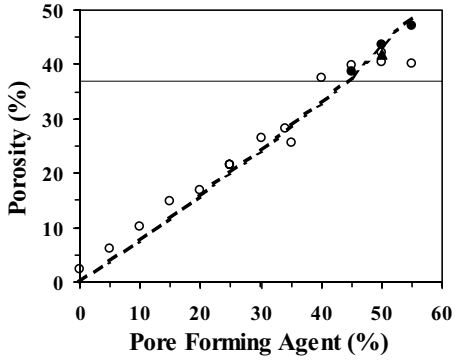

Fig. 4. Volume fraction of porosity after sintering vs. PFA content. Monolithic laminates: (○) corn starch; laminar composites: (●) corn starch, (▲) graphite platelets. The dotted line corresponds to the equation from Slamovich and Lange.[14] The solid line corresponds to the critical porosity for crack deflection according to Refs. 7,8.

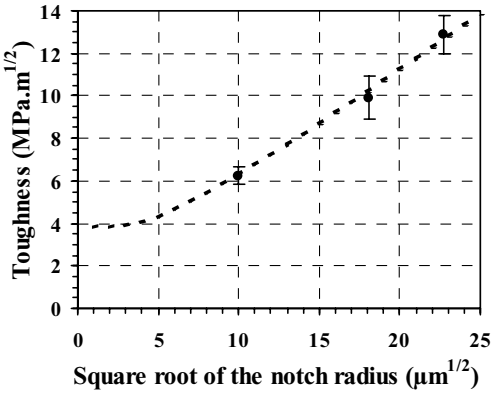

Fig. 5. Dependence of toughness measured by the SENB-S method on the square root of the notch radius for dense monolithic laminates. The doted curve corresponds to Eq. (5) with $Y = 1.12$ and $\delta a = 10\,\mu$m.

3. Experimental procedures

Young's modulus, E, was calculated from the measurement of the velocity of longitudinal, V_L, and shear, V_S, ultrasonic waves using a pulse echo overlap technique in the approximation of an homogeneous isotropic infinite medium:[15]

$$E = \rho V_S^2 \left[\frac{3V_L^2 - 4V_S^2}{V_L^2 - V_S^2} \right] \tag{3}$$

where ρ is the density.

The modulus of rupture, σ_R, was measured in 3-point bending at a cross-head speed of 0.2 mm/min.

The experimental method for the toughness determination must be applicable to highly porous materials, that eliminates indentation based methods. So, the single edge notch beam-saw cut method (SENB-S) was selected. Another reason for this choice was that, analysing the results of an European round robin test, Damani et al.[16] have concluded that this method seemed to deliver the most reproducible results. The toughness was calculated from the measurement of the modulus of rupture in 3-point bending and the depth of the initial notch, a, according to the following equation:[17]

$$K_{1C}^{SENB} = \sigma_R \sqrt{a} \sum_{i=0}^{4} \left[A_i \left(\frac{a}{w} \right)^i \right] \tag{4}$$

where w is the height of the sample and A_i are coefficients given by: $A_0 = 1.9 + 0.0075L/w$; $A_1 = -3.39 + 0.08L/w$; $A_2 = 15.4 - 0.2175L/w$; $A_3 = -26.24 + 0.1825L/w$; $A_4 = 26.38 - 0.145L/w$ with L being the span.

However, this method leads to an overestimated value of the toughness when the notch root value, r, is larger than a critical value of the order of a few microns. Damani et al.[16] suggested and verified experimentally that the true toughness, K_{1C}^T, is related to the measured toughness by the relation:

$$K_{1C}^T = K_{1C}^{SENB} \tanh\left(2Y \sqrt{\frac{\delta a}{r}} \right) \tag{5}$$

where Y is a geometric correction factor and δa is the size of the small defect at the notch-tip, under the influence of the stress interaction field of the notch.

In order to assess if it was possible to use Eq. (5) for the correction of our experimental data, the toughness of SiC dense monolith was measured for three different root radii (100, 300 and 1000 μm) and fitted by Eq. (5). In the case of this dense, fine grained material, the defect at the notch-tip was assumed to result from machining, i.e., an edge crack configuration ($Y = 1.12$) and machining scratches, δa, of 10 μm were adopted.[16] Fig. 5 shows that a good agreement was obtained, giving an extrapolated value at $r = 0$ of 3.82 MPa m$^{1/2}$, which falls nicely in the values between 3 and 4 MPa m$^{1/2}$ usually obtained for α-SiC with this kind of microstructure. In the case of the porous monoliths, the crack defects at the notch-tip were assumed to have also an edge crack configuration and their size was taken equal to 10 μm or to the mean average Férêt diameter of the porosity when it was greater than 10 μm.[18]

The fracture energy was calculated from the measurements of the toughness and Young's modulus from the relation:

$$G_{1C} = \frac{K_{1C}^2}{E} \tag{6}$$

4. Mechanical properties

The experimental data for dense and porous monoliths are reported in Fig. 6. Seven specimens were used for the determination of the modulus of rupture and of the toughness.

The data were fitted by a $(1 - P)^m$ form, since Blanks et al.[7] have obtained for SiC a good description of Young's

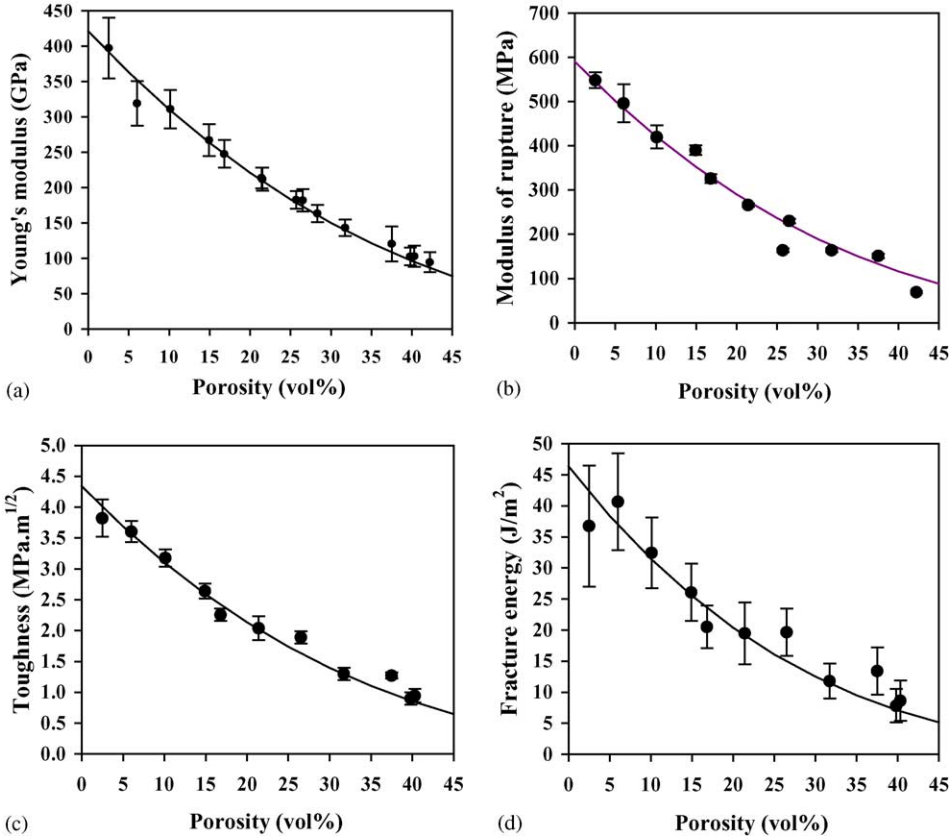

Fig. 6. Dependence on porosity of the mechanical properties of monolithic laminates (PFA = CS). (a) Young's modulus; (b) modulus of rupture; (c) toughness; (d) fracture energy. The solid lines correspond to the best fit with Wagh's equations.

modulus with $E_P = E_0(1-P)^2$. Such an equation was also established by Wagh et al.[19] for a model derived from an previous analytical one developed by Wong et al.[20] in efforts to explain charge and mass transport through the random pore structure of rocks. The assumed ceramic structure is a three-dimensional, intertwined, continuous network of material chains and open-pore channels. This assumption is based on the fact that it is possible to fabricate ceramics with a very high porosity, as high as 93%,[21] and that open pores exist even at very low porosity (6%). This is consistent with the mainly open nature of the porosity in the present materials where the pores introduced by the pore forming agents are interconnected by small channels.[13]

The fitting parameters obtained using a classical mean square method, are reported in Table 2.

The m_E parameter (2.68), is greater than the value of 2 obtained experimentally by Blanks et al.[7] According to Wagh et al. this value of 2 is characteristic of ceramics densified without additives or applied pressure. However, for materials hot-pressed or densified using sintering aids leading to an intergranular glassy phase, m_E takes value greater than 2.

Table 2
Fitting parameters for the mechanical properties using Wagh's model

Property	Extrapolated at $P = 0$	m	Correlation factor
E (GPa)	407 ± 7	2.68 ± 0.08	0.995
σ_R (MPa)	590 ± 15	3.18	0.98
K_{1C} (MPa m$^{1/2}$)	4.34 ± 0.09	3.18	0.99
G_{1C} (J/m^2)	46.4 ± 2.0	3.68	0.96

Wagh et al.[22] derived, for the fracture properties, power laws with different exponents connected together by:

$$m_{\sigma_R} = m_{K_{1C}} = m_E + 0.5 \text{ and } m_{G_{1C}} = m_E + 1$$

The results from fits done with the exponents put at their theoretical values are reported in Table 2. The correlation factors are fairly good.

The model developed by Wagh et al.[19,22] that takes into account the tortuosity of the porosity, describes the whole set of our experimental data of the mechanical properties over the entire porosity range (from $P = 0\%$ to $P = 42\%$) and appears to be well adapted to the present porosity morphology.

5. Fracture behaviour

5.1. Experimental results

The fracture behaviour of the laminar composite (LC) was studied in 3-point bending for unnotched and notched

Table 3
Laminar composites

Pore forming agent	PFA content (vol.%)	Porosity (vol.%)	Laminar composite sequences[a]
Corn starch	55	47 (42)[b]	1/1–2/1–1/2
	50	43.5 (40)[b]	1/1–2/2–3/1–2/1–1/2
	45	40	1/1
	34	28	1/1
	25	21	1/1
Graphite platelets	50	41	1/1–2/1–1/2

[a] For a given sequence, the numbers refer to the number of tapes stacked to make one layer and indicate the relative thickness of the dense/porous layers. The first number concerns the dense layers, the second one the porous ones (see Section 2.2).
[b] The values into brackets correspond to the porous monoliths whereas the others are the values in the porous interlayers of the composites.

samples. The cross-head displacement rate was varied from 0.5 to 0.004 mm/min to test a possible effect of the solicitation rate. The role of the pore morphology was illustrated by comparing the behaviour of composites obtained using corn starch (CSLC) and graphite platelets (GPLC) as pore forming agent. The different materials and architectures are listed in Table 3.

Typical load–deflection curves for CSLC and GPLC are reported in Fig. 7. For all the materials, the load remains linear up to the peak load, at which point a crack initiates at some surface defects and grows quickly in the through thickness direction.

According to Clegg's group,[7,8] crack deflection should be observed when relation 2 is fulfilled, i.e., when $G_P/G_S(1-P)$ becomes lower than 0.57, and extensive deflection must occur when this ratio is lower than 0.4, that corresponds to porosity higher than 37 and 44%, respectively (see Fig. 8 in Ref. 7). Using the parameters from Wagh's model (Table 2), the corresponding values of porosity for the present materials are 19 and 33%, respectively. Then, from Fig. 8, where $G_P/G_S(1-P)$, calculated from the experimental data reported in Section 4, is plotted versus the porosity of the porous layers, it should be the case at least for the specimens where the porous layers have a porosity equal to 40, 43.5 and 47%.

However, in the case of CSLC, whatever the porosity level, the cross-head speed or the architecture, the rupture was catastrophic with no increase in the work of fracture. SEM micrographs of the side surfaces are shown in Fig. 9. For porosity levels up to 30%, the surface of rupture is flat and is not affected by the alternation of dense/porous layers. For larger porosity levels, whereas the crack propagates perpendicularly through the dense layers, its direction changes progressively in the porous layers, but, the lengths of deflection are extremely short, of the order of 100 μm or less, except for the architecture with a dense to porous thickness ratio of 3 where deflections of 300 μm are observed. Then, the crack kinks out of the porous interphase when it reaches the porous/dense interface without inducing delamination.

In the case of GPLC, where the pores are elongated and lie roughly parallel to the interfaces, the occurrence of a secondary load peak (see curves B in Fig. 7) indicates that the penetrating crack was effectively arrested, that allowed the measured load to rise again until a new crack formed. The deflection in curve B1 corresponds to the cross-head displacement whereas the deflection in curve B2 corresponds to the displacement of the outer tensile surface (see the schematic illustration in Fig. 7). The difference between the deflection

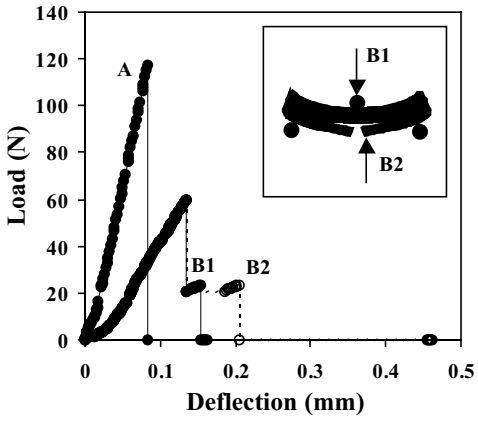

Fig. 7. Typical load–displacement curves in 3-point bend test of laminar composites. A: CSLC (sequence 1/1, $P = 43.5\%$); B: GPLC (sequence 1/1, $P = 41\%$). The deflection for B1 corresponds to the cross-head displacement; that for B2 corresponds to the displacement of the outer tensile layer (see explanation at the end of Section 5.1).

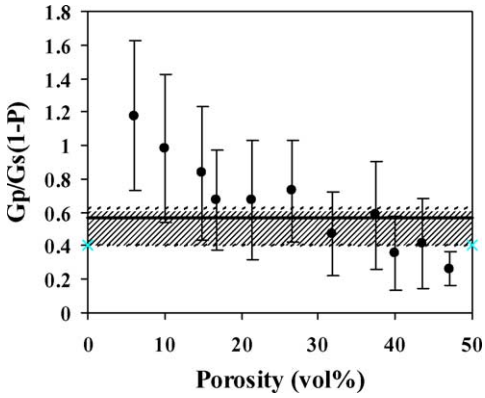

Fig. 8. $G_P/G_S(1-P)$ vs. porosity of the porous layers (corn starch). The solid line corresponds to $G_P/G_S(1-P) = 0.57$ (Eq. (2)). The shadowed band divides the graph in an upper region where crack does not deflect and a lower region where crack did deflect according to Blanks et al.[7]

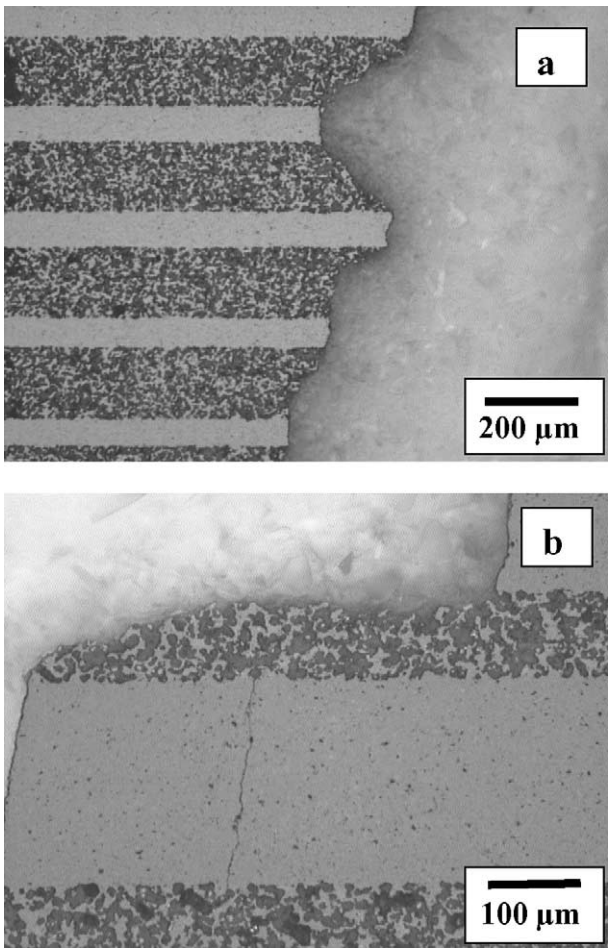

Fig. 9. SEM micrographs of side surfaces of representative broken laminar composites (CSLC). (a) $P = 47$ vol.%, sequence 1/2; (b) $P = 43.5$ vol.%, sequence 3/1. Though the crack changes direction, it kinks out of the porous interlayer giving no useful toughening.

in the two curves reflects the opening of a crack in a plane perpendicular to the applied load and corresponds to a delamination.

5.2. Discussion

Contrary to was expected, deflection was not observed for specimens that meet relation 2. As the only obvious difference between our samples and those of Blanks et al.[7] is that Blanks' ones were densified by solid state sintering whereas ours are densified by liquid phase sintering, the lack of crack deflection in our specimens might be linked to the presence of an intergranular amorphous phase. An argument that might support this hypothesis is the fact that, whereas in solid state sintered SiC crack propagation is transgranular,[23] the propagation in the present case is intergranular (Fig. 10) that suggests an influence of the intergranular amorphous films on the mechanical behaviour.

However, the comparison of the behaviour of the present laminar composites with those of the SiC/SiC–graphite laminates studied by Vandeperre and Van Der Biest[24] can also shed light on our results. These authors have fabricated, by electrophoretic deposition, laminar composites with alternating layers of dense β-SiC and β-SiC containing different amounts of graphite (21, 34, 52 and 76 vol.% C, respectively labelled types B, C, D and E). The mechanical behaviour, tested in 3-point bending, showed no crack deflection for the two lowest graphite contents (types B and C) but only slight deviation from the straight-through path. In the case of the composite with layers containing 52 vol.% of graphite, some specimens did not show a completely brittle failure but exhibited a load–deflection curve similar to that observed for the GPLC specimens of the present work. Crack deflection occurred reliably only for type E material (i.e., the highest graphite content). The fracture energy of CSLC is compared with that of the materials studied by Vandeperre and Van Der Biest in Fig. 11. The fracture energy of their type D interlayers (52 vol.% C) is the same as that of our highest porous CSLC samples and the behaviour of the correspond-

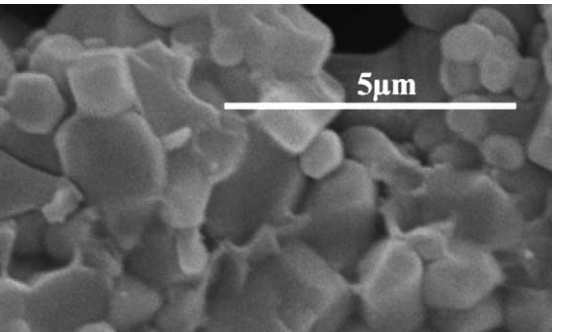

Fig. 10. SEM micrograph of typical surface of fracture showing that the rupture is intergranular. Monolithic laminate, PFA = CS, porosity = 15 vol.%.

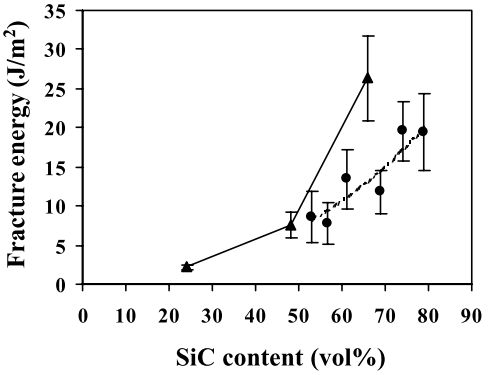

Fig. 11. Fracture energy of porous SiC layers (●) in CSLC as a function of the volume fraction of SiC compared to that of SiC+graphite interfaces (▲) in SiC/SiC–graphite laminar composites.[24]

ing laminar composites mimics either that of CSLC or that of GPLC.

Let us now compare our materials with laminar composites in the Si_3N_4 system (i.e., materials densified by liquid phase sintering through the addition of 6 vol.% of yttria) that were studied by Kovar et al.[3] Five grades of weak layers were obtained from mixtures of Si_3N_4 and hexagonal BN: 20, 50, 75, 90 and 100 vol.% of boron nitride. The load–deflection curves showed brittle failure up to 50 vol.% BN. For this last BN content the delaminations are reported to be extremely short, less than 100 μm. Substantial crack deflection and delamination started to be observed for BN content in the weak interlayers equal to 75 vol.%.

Due to the low cohesive force between graphite and SiC or between BN and Si_3N_4 grains, it could be assumed that the graphite or BN platelets play a role similar to the pores resulting from the pyrolysis of the graphite platelets in the GPLC specimens. In this respect, it appears that crack deflection reliably occurs only for volume content significantly greater than the 37 vol.% derived by Blanks et al. Unfortunately, we were not able to process layers with a porosity higher than 47% because the quantity of gas evolving from the burn out of the pore forming agent was too large and led to cracking and swelling of the materials. However, in the light of the above comparison with SiC/SiC–graphite and Si_3N_4/Si_3N_4–BN composites, our opinion is that it is unlikely that the difference in the densification mechanism could be the reason why Blanks' specimens showed crack deflection and not ours. Unfortunately, a more in-depth comparison of the two sets of dense/porous laminates could not be performed because of the lack of information on the microstructure of the materials fabricated by Blanks and his co-workers.

6. Conclusion

SiC materials have been fabricated by stacking tape cast sheets and densification of the stack by liquid phase sintering (YAG-alumina eutectic). Controlled porosity was introduced by the incorporation of pore forming agent in the slurry. Two types of samples have been prepared: monolithic blocks to determine the mechanical properties and alternate dense/porous laminates to test the ability to increase the work of rupture by promoting crack deflection in the weak interlayers.

The dependence on porosity of the mechanical properties (Young's modulus, modulus of rupture, toughness and fracture energy) has been found to be well fitted on the entire range of porosity (0–42%) by the set of equations proposed by Wagh et al.[19,22] from a model that takes into account the tortuosity of the porosity.

Though laminates with weak interlayers having a porosity higher than the critical level required for crack deflection according to Clegg's group were fabricated, no significant delaminations were observed. However, the behaviour of the present composites has been shown to be consistent with the behaviour observed for SiC/SiC–graphite[24] and Si_3N_4/Si_3N_4–BN[3] composites. Our opinion is that porosity levels higher than the critical value proposed by Blanks et al.[7] are needed for crack deflection to occur reliably in dense/porous laminar composites.

References

1. Clegg, W. J., Kendall, K., Alford, N. M., Birchall, D. and Button, T. W., A simple way to make tough ceramics. *Nature* 1990, **347**, 455–457.
2. Liu, H. and Hsu, S. M., Fracture behavior of multilayer silicon nitride/boron nitride ceramics. *J. Am. Ceram. Soc.* 1996, **79**, 2452–2457.
3. Kovar, D., Thouless, M. D. and Halloran, J. W., Crack deflection and propagation in layered silicon nitride/boron nitride ceramics. *J. Am. Ceram. Soc.* 1998, **81**, 1004–1012.
4. Mawdsley, J. R., Kovar, D. and Halloran, J. W., Fracture behavior of alumina/monazite multiplayer laminates. *J. Am. Ceram. Soc.* 2000, **83**, 802–808.
5. King, T. T. and Cooper, R. F., Ambient-temperature mechanical response of alumina-fluoromica laminates. *J. Am. Ceram. Soc.* 1994, **77**, 1699–1705.
6. Zhang, G.-J., Yue, X. M. and Watanabe, T., High-temperature multilayer composites with superplastic interlayers. *J. Am. Ceram. Soc.* 1999, **82**, 3257–3259.
7. Blanks, K. S., Kristoffersson, A., Carlström, E. and Clegg, W. J., Crack deflection in ceramic laminates using porous interlayers. *J. Eur. Ceram. Soc.* 1998, **18**, 1945–1951.
8. Davis, J. B., Kristoffersson, A., Carlström, E. and Clegg, W. J., Fabrication and crack deflection in ceramic laminates with porous interlayers. *J. Am. Ceram. Soc.* 2000, **83**, 2369–2374.
9. Howard, S. J., Stewart, R. A. and Clegg, W. J., Delamination of ceramic laminates due to residual thermal stresses. In *Key Engineering Materials, Vols 116–117*, ed. T. W. Clyne. Trans. Tech. Publications, Switzerland, 1996, pp. 331–350.
10. He, M.-Y. and Hutchinson, J. W., Kinking of a crack out of an interface. *J. Appl. Mech.* 1989, **56**, 270–278.
11. Gong, S.-X. and Horii, H., General solution to the problem of microcracks near the tip of a main crack. *J. Mech. Phys. Solids* 1989, **37**(1), 27–46.
12. Alford, N. M., Birchall, J. D. and Kendall, K., High strength ceramics through colloidal control to remove defects. *Nature* 1987, **330**, 51–53.
13. Reynaud, C., Thevenot, F. and Chartier, T., Processing and microstructure of SiC laminar composites. *Int. J. Refract. Met. Hard Mater.* 2000, **19**, 425–435.
14. Slamovich, E. B. and Lange, F. F., Densification of large pores: I. Experiments. *J. Am. Ceram. Soc.* 1992, **75**, 2498–2508.
15. Mc Skimmin, H. J., Measurement of ultrasonic wave velocities for solids in the frequency range 100 to 500 MHz. *J. Acoust. Soc. Am.* 1960, **34**, 404–409.
16. Damani, R. J., Gstrein, R. and Danzer, R., Critical notch-root radius effect in SENB-S fracture toughness testing. *J. Eur. Ceram. Soc.* 1996, **16**, 695–702.
17. Jordan, Y., *Elaboration et Caractérisation de Composites Dispersoïdes Base Alumine-zircone à Vocation Thermodynamique*. Ph.D. thesis, ENSM-SE/INSA Lyon, Saint-Etienne, France, 1991.
18. Reynaud, C., *Céramiques Lamellaires Monolithiques et Composites en Carbure de Silicium*. Ph.D. thesis, ENSM-SE/INPG, Saint-Etienne, France, 2002.

19. Wagh, A. S., Poeppel, R. B. and Singh, J. P., Open pore description of mechanical properties of ceramics. *J. Mater. Sci.* 1991, **26**, 3862–3868.
20. Wong, P., Koplik, J. and Tomanic, J. P., Conductivity and permeability of rocks. *Phys. Rev. B* 1984, **30**, 6606–6614.
21. Ashby, M. F., The mechanical properties of cellular solids. *Metall. Trans. A* 1983, **14**, 1755–1768.
22. Wagh, A. S., Singh, J. P. and Poeppel, R. B., Dependence of ceramic fracture properties on porosity. *J. Mater. Sci.* 1993, **28**, 3589–3593.
23. Govila, R. K., Phenomenology of fracture in sintered alpha silicon carbide. *J. Mater. Sci.* 1984, **19**, 2111–2120.
24. Vandeperre, L. and Van Der Biest, O., Composite SiC–graphite interlayers for crack deflection in ceramic laminates. *Silic. Ind.* 1998, **63**, 39–43.